Hydrodynamic Lyapunov modes and strong stochasticity threshold in the dynamic *XY* model: An alternative scenario

Hong-liu Yang* and Günter Radons†
Institute of Physics, Chemnitz University of Technology, D-09107 Chemnitz, Germany
(Received 2 October 2007; published 17 January 2008)

Crossover from weak to strong chaos in high-dimensional Hamiltonian systems at the strong stochasticity threshold (SST) was anticipated to indicate a global transition in the geometric structure of phase space. Our recent study of Fermi-Pasta-Ulam models showed that corresponding to this transition the energy density dependence of all Lyapunov exponents is identical apart from a scaling factor. The current investigation of the dynamic *XY* model discovers an alternative scenario for the energy dependence of the system dynamics at SSTs. Though similar in tendency, the Lyapunov exponents now show individually different energy dependencies except in the near-harmonic regime. Such a finding restricts the use of indices such as the largest Lyapunov exponent and the Ricci curvatures to characterize the global transition in the dynamics of high-dimensional Hamiltonian systems. These observations are consistent with our conjecture that the quasi-isotropy assumption works well only when parametric resonances are the dominant sources of dynamical instabilities. Moreover, numerical simulations demonstrate the existence of hydrodynamical Lyapunov modes (HLMs) in the dynamic *XY* model and show that corresponding to the crossover in the Lyapunov exponents there is also a smooth transition in the energy density dependence of significance measures of HLMs. In particular, our numerical results confirm that strong chaos is essential for the appearance of HLMs.

DOI: 10.1103/PhysRevE.77.016203 PACS number(s): 05.45.Jn, 05.20.−y, 05.45.Pq, 05.45.Xt

I. INTRODUCTION

During the past decades one observes a continuously growing research interest in the nonlinear dynamics of high-dimensional Hamiltonian systems. They are partially motivated by the hope to explain some fundamental issues at the basis of statistical mechanics from the point of view of nonlinear dynamics [1–6]. One well-known example is the numerical experiment performed by Fermi, Pasta, and Ulam (FPU) in 1955 [7] attempting to check whether a high-dimensional Hamiltonian system starting from nonequilibrium initial conditions would relax to equilibrium, eventually. Their observation of the recurrent flow of energy among normal modes strongly challenged the validity of statistical mechanics in high-dimensional nonintegrable Hamiltonian systems and initiated a lot of research efforts during the past half century [8].

One promising explanation to the FPU puzzle, which emerged, relates it to the existence of a threshold energy for stochasticity or equipartition. Such a point of view is consistent with the Kolmogorov-Arnold-Moser (KAM) theory [9] and was supported by some early numerical experiments [10–12]. Benefiting from the accelerating development of the power of modern computers, further numerical work was carried out in the last two decades clarifying that the previously claimed threshold does not characterize a transition from regular to chaotic states but a smooth transition in the system dynamics from weak to strong chaos [13,14]. Therefore, it is referred to as the strong stochasticity threshold (SST) in the literature [14]. Relaxation times and the largest Lyapunov exponent show different scaling behavior in the regimes beyond and below the SST [13,14]. Similar results were reported for a large number of systems [15–18] and indicate that the existence of the SST is a quite general aspect of Hamiltonian systems with many degrees of freedom.

In a series of recent papers [19–23] Pettini and coworkers developed the geometric theory of Hamiltonian chaos. Within such a frame, trajectories of Hamiltonian systems correspond to the geodesics of a Riemannian manifold with a suitable metric. Dynamic instability of trajectories is related to the curvature properties of the ambient manifold. More precisely, it is governed by the Jacobi-Levi-Civita equation for the geodesic variations. As a main tool for tackling chaos in Hamiltonian systems, such a tensor equation is too complex to be handled for high dimensional systems. Approximations are often necessary to reduce the tensor equation of Jacobi-Levi-Civita to some simpler scalar equations. Instead of the Riemannian curvature tensor in the Jacobi-Levi-Civita equation, the simpler scalar curvature or Ricci curvature is used as index of geometric changes in the structure of the ambient manifold. Especially, the transition in the system dynamics at the SST is demonstrated to indicate a dramatic change in the geometric structure of configuration space [19,20].

Recently, Posch and co-workers discovered that some interesting information is contained in Lyapunov vectors of a high dimensional system with certain continuous symmetries. They demonstrated the existence of wavelike collective structures in Lyapunov vectors associated with near-zero Lyapunov exponents [24]. They were called hydrodynamic Lyapunov modes (HLMs) owing to their long wavelength and long relaxation time nature. Due to the potential importance for understanding the fundamental problems of statistical mechanics from the point of view of nonlinear dynamics [25–35] HLMs have already been investigated in various

*hongliu.yang@physik.tu-chemnitz.de
†radons@physik.tu-chemnitz.de

systems ranging from many-particle systems with hard-core [25,29] or soft-potential interaction [31–33], products of random matrices [26], and coupled map lattices [34] to the Kuramato-Shivashinsky equation [35].

We reported in a recent paper on the variation of Lyapunov spectra and hydrodynamic Lyapunov modes (HLMs) in FPU models in connection with the SST [36]. We found that all Lyapunov exponents as function of the energy density vary in a similar way. This means that the data for the energy density dependence of all Lyapunov exponents collapse to a master curve after a simple rescaling. This observation on one hand supports the anticipation that the smooth transition in the system dynamics at the SST reflects a global change in the geometric structure of phase space, and it explains on the other hand why the approximation of quasi-isotropy works very well in the analytical estimation of the largest Lyapunov exponent in FPU models [22]. Corresponding to such a change in the Lyapunov exponents, HLMs are found to behave differently in the regimes of weak and strong chaos, respectively. Especially strong chaos is found to be an essential factor for the appearance of significant HLMs.

A known fact from previous investigations is that in some systems like the dynamic XY model the occurrence of negative curvature acts as an additional source of dynamical instability. Moreover, the analytical estimation of the largest Lyapunov exponent based on the quasi-isotropy approximation shows rather large deviations from the numerical results in contrast to its success in FPU models [22,23]. The main issue to be addressed in the present contribution is to find out the geometric origin and further indications of the difference between XY-spin systems and FPU models. We study the energy density dependence of the whole Lyapunov spectrum and HLMs in the dynamic XY model in comparison with FPU models [37–39]. We found that, although all Lyapunov exponents experience a characteristic change in their energy density dependence at the SST, they differ in their individual energy dependence. These observations indicate the existence of alternative scenarios in the change of the geometric structure of configuration space in connection with the SST. HLMs are found to exhibit different behavior in the regimes of weak and strong chaos. The essence of strong chaos for the existence of significant HLMs is confirmed again by our simulations.

The remainder of the paper is organized as follows. The model system under investigation and the details of the numerical simulations are given in Sec. II. In order to facilitate comparison, we will present in Sec. III the main change in the dynamics of the XY model in connection with SST. In Sec. IV the results of numerical simulations with respect to the variation of the Lyapunov spectrum and HLMs will be presented. Finally we will summarize the main results and end the paper with a short discussion. Complementary to the results reported in the main body of this paper, we show in the Appendix the results for the lattice ϕ^4 model. The scenario for the variation of the Lyapunov exponents there is rather similar to that of FPU models.

II. MODEL AND DETAILS OF NUMERICAL SIMULATIONS

Our one-dimensional dynamic XY model is described by a Hamiltonian of the form [37–39]

$$H = \sum_{l=1}^{L} \left[\frac{p_l^2}{2} + V(\theta_{l+1} - \theta_l) \right], \tag{1}$$

where θ_l denotes the displacement of the lth particle from its equilibrium position, $p_l = \dot{\theta}_l$ is the conjugate momentum, and periodic boundary conditions $\theta_{l+L} = \theta_l$ are used. The potential $V(z)$ is of the form

$$V(z) = 1 - \cos z. \tag{2}$$

Note the inclusion of the additional kinetic energy term in Hamiltonian Eq. (1) at variance from the conventional XY model. The energy density $\epsilon \equiv E/L$, where E is the total energy, is used as a control parameter to investigate the variation in Lyapunov characteristics.

One may recognize that the Hamiltonian Eq. (1) is invariant under the variable transformation $\theta_l' = \theta_l + c$ with an arbitrary constant c, since only internal forces among particles are present there. In consequence, the total momentum $P \equiv \sum_{l=1}^{L} p_l$ is conserved. The appearance of HLMs is just due to the spontaneous breaking of such a symmetry in the tangent space dynamics.

The equations of motion, which can be easily derived from the given Hamiltonian, are integrated with a fourth order Runge-Kutta algorithm [40]. The so-called standard method is adopted to calculate the Lyapunov exponents and Lyapunov vectors [41].

To detect the coherent structures in Lyapunov vectors and to characterize the hydrodynamic Lyapunov modes quantitatively, we have introduced the correlation function theory for Lyapunov vectors [31,32,34]. Lets recall it briefly here. A dynamical variable called *LV fluctuation density* is defined as

$$\mathcal{U}^{(\alpha)}(r,t) = \sum_{l=1}^{L} \delta\theta_t^{(\alpha)l} \delta(r - r_l), \tag{3}$$

where r_l is the position coordinate of the lth particle and $\{\delta\theta_t^{(\alpha)l}\}$ is the coordinate component of the αth Lyapunov vector for the lth particle. The position coordinate is simply $r_l \equiv l \cdot a$ for the lattice models used here. We set the lattice constant $a = 1$ throughout the remainder of this paper.

The so-called static LV structure factor is defined as

$$S_u^{(\alpha\alpha)}(k) = \langle \mathcal{U}_k^{(\alpha)}(t) \mathcal{U}_{-k}^{(\alpha)}(t) \rangle, \tag{4}$$

where $\langle \cdots \rangle$ represents the time average and $\mathcal{U}_k^{(\alpha)}(t) = \int \mathcal{U}^{(\alpha)} \times (r,t) e^{-ik\cdot r} dr = \sum_{l=1}^{L} \delta\theta_t^{(\alpha)l} e^{-ik\cdot r_l}$ is the spatial Fourier transformation of $\mathcal{U}^{(\alpha)}(r,t)$. As can be easily seen from Eq. (4), the static LV structure factor is nothing but the spatial Fourier spectrum of the LV fluctuation density $\mathcal{U}^{(\alpha)}(r,t)$. Therefore it is suited for the characterization of the spatial structure of Lyapunov vectors.

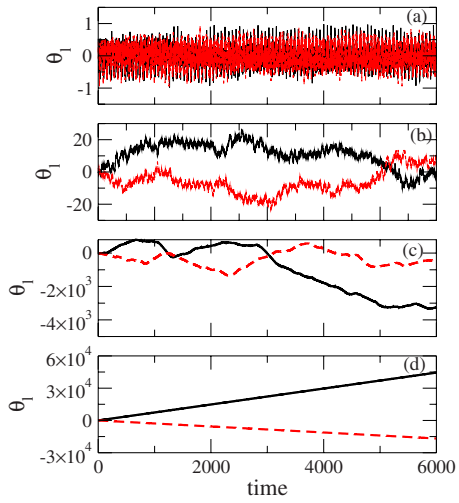

FIG. 1. (Color online) Time evolution of the coordinate θ_l for two randomly selected elements for four cases with energy density (a) ϵ=0.04, (b) 0.4, (c) 4, and (d) 40, respectively. Notice the change in the system dynamics with increasing energy density.

III. TRANSITIONS IN THE DYNAMICS OF THE *XY* MODEL

We present the main change in the dynamics of the dynamic *XY* model with variation of the energy density. The qualitative change in the system dynamics will help to coordinate transitions in Lyapunov characteristics.

The time evolutions of the coordinate θ_l for two randomly selected elements are presented in Fig. 1 for various energy densities. When the energy density is low enough, all elements in the lattice just liberate around their equilibrium positions [see panel (a)]. With increasing the energy density beyond a certain threshold value, the dynamics of elements show intermittent switching between liberation and rotation [see panel (b)]. The probability for rotational motion increases and the coherence among dynamics of different elements becomes weaker with increasing the energy density [see panel (c)]. Finally all elements rotate nearly freely as the energy density is large enough [see panel (d)]. Such observations are consistent with the existence of two integrable limits in this system, the harmonic limit at small energy density and the free rotation limit at high energy density respectively [16].

We show in Fig. 2 the variation of the quantity $\langle \theta_l^2 \rangle$ with time t, where $\langle \cdots \rangle$ represents an average over elements. Distinct long-time behavior is observed for the cases corresponding to Fig. 1. Fitting the evolution of $\langle \theta_l^2 \rangle$ with t to a power law function $\langle \theta_l^2 \rangle \sim t^{\gamma}$ yields a characteristic exponent γ for the system dynamics. The variation of γ with the energy density ϵ is shown in Fig. 2(b). Three regimes can roughly be classified, the near-harmonic regime $\epsilon < \epsilon_{c1} \approx 0.14$ with $\gamma \approx 0$, the free rotation regime $\epsilon > \epsilon_{c2} \approx 10$ with $\gamma \approx 2$ and the strong chaotic regime $\epsilon_{c1} < \epsilon < \epsilon_{c2}$ with $\gamma \approx 1$. The threshold values ϵ_{c1} and ϵ_{c2} are in good agreement with the previous analytical estimation in [16] by using Gibbsian estimates of dynamical observables.

The variation of the kinetic temperature $T \equiv \langle p_l^2 \rangle$ and the potential energy density $v \equiv V/N$ with the energy density ϵ is shown in Fig. 3. Both quantities exhibit a crossover at $\epsilon_M \approx 1$. In the low energy regime $\epsilon < \epsilon_M$, one has $T = \epsilon$ and $v = 0.5\epsilon$ which implies the equal partition of the total energy between kinetic and potential energy parts. In the high energy regime $\epsilon > \epsilon_M$, the potential energy density tends to saturate to a constant 1.0 while the temperature T and the kinetic energy density increase linearly with ϵ. Inspection of the system dynamics shows that it is dominated by libration and rotation in the regime below and beyond the threshold value ϵ_M, respectively.

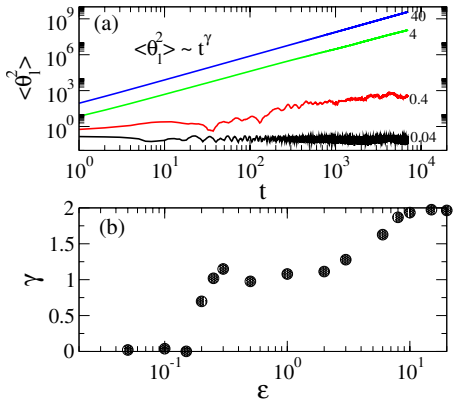

FIG. 2. (Color online) (a) Time evolution of the quantity $\langle \theta_l^2 \rangle$ for the corresponding cases shown in Fig. 1. (b) The variation of the exponent γ with the energy density ϵ. Notice the existence of three regimes with $\gamma \approx 0$, $\gamma \approx 1$, and $\gamma \approx 2$, respectively. The two threshold values are $\epsilon_{c1} \approx 0.14$ and $\epsilon_{c2} \approx 10$.

In summary, the dynamic *XY* model has four different types of states in the regimes separated by the three threshold values. They are the weak chaotic state dominated by libration (WL) with $\epsilon < \epsilon_{c1}$, the strong chaotic state dominated by libration (SL) with $\epsilon_{c1} < \epsilon < \epsilon_M$, the strong chaotic state dominated by rotation (SR) with $\epsilon_M < \epsilon < \epsilon_{c2}$, and the weak chaotic state dominated by rotation (WR) with $\epsilon > \epsilon_{c2}$. Three transitions between these chaotic states take place at the three threshold values ϵ_{c1}, ϵ_{c2} and ϵ_M respectively. We will show below the change of the Lyapunov characteristics corresponding to these transitions in the system dynamics.

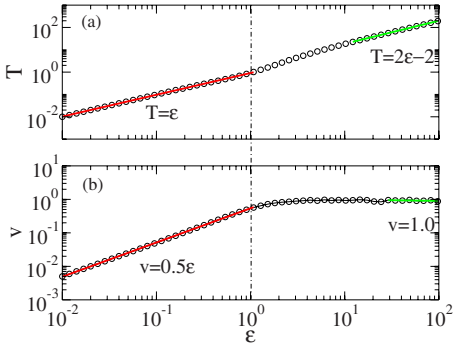

FIG. 3. (Color online) Energy density dependence of (a) the temperature T and (b) the potential energy density v. Both quantities change their behavior in a regime around $\epsilon_M \approx 1$.

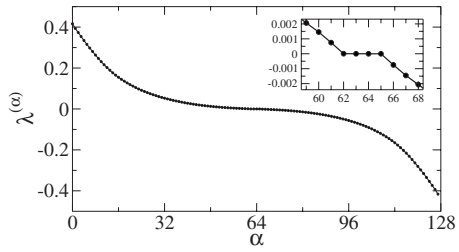

FIG. 4. Lyapunov spectrum of a case with $\epsilon=4$. Due to the Hamiltonian nature of the system dynamics the Lyapunov spectrum has the symmetry $\lambda^{(\alpha)}=-\lambda^{(2L-1-\alpha)}$. As can be seen from the inset, the system has four zero-value Lyapunov exponents. The system size used here is $L=64$.

IV. NUMERICAL RESULTS FOR LYAPUNOV SPECTRA AND HYDRODYNAMIC LYAPUNOV MODES

A. Transitions in Lyapunov exponents

The Lyapunov spectrum for the case $\epsilon=4$ is shown in Fig. 4. It has the symmetry $\lambda^{(\alpha)}=-\lambda^{(2L-1-\alpha)}$ in consequence of the symplectic structure of Hamiltonian systems. As can be seen from the inset, the system has four zero-value Lyapunov exponents, which are related to the space and time translational invariance symmetries of the system and the associated conserved quantities, the total energy and the total momentum. The symmetry of the spectrum and the appearance of four zero Lyapunov exponents also demonstrates that our integration algorithm keeps the symplectic structure of the investigated system very well.

We present in Fig. 5 the change of the largest Lyapunov exponent $\lambda^{(0)}$ with increasing energy density ϵ. In the low energy regime $\epsilon<\epsilon_{c1}$, the data can be fitted very well by a power law function $\lambda^{(0)}\sim\epsilon^{\beta}$ with $\beta\simeq 2.0$ [22]. Similar behavior has been observed in the FPU models in the low energy regime, which turns out to be a characteristic feature of near-harmonic dynamics. The ascent of $\lambda^{(0)}$ with ϵ first becomes much steeper and then decreases as ϵ increases beyond the value ϵ_{c1}. It reaches a maximum around $\epsilon_M\approx 1$. With further increasing ϵ, $\lambda^{(0)}$ starts to decrease. But the rate of descent is much smaller than the rates of ascent in other regimes. The profile of the overall variation of $\lambda^{(0)}$ forms a kneelike structure (see Fig. 5).

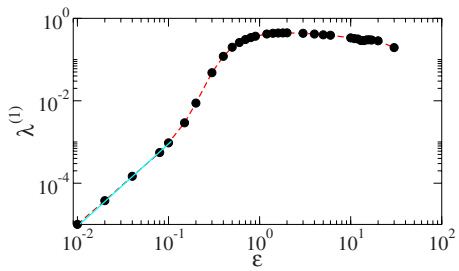

FIG. 5. (Color online) Largest Lyapunov exponent $\lambda^{(0)}$ vs energy density ϵ for the dynamic XY model. The ϵ dependence of $\lambda^{(0)}$ is fitted to a power law with the exponent 2.0 in the low-energy regime $\epsilon<\epsilon_{c1}\approx 0.14$.

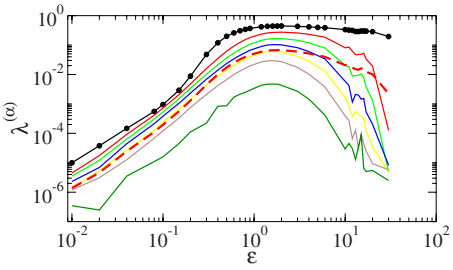

FIG. 6. (Color online) ϵ dependence of typical Lyapunov exponents in the positive branch of the Lyapunov spectrum for the dynamic XY model. Here, α takes the value from 0 to 60 with the increment 10 (from top to bottom). The density of the Kolmogorov-Sinai entropy $\rho_h\equiv h_{\mathrm{KS}}/N$ is plotted as a dashed line. Obviously, except in the low-energy regime $\epsilon<\epsilon_{c1}$ the profiles of change of all Lyapunov exponents are different from each other.

Besides the above-mentioned change in the ϵ dependence of the largest Lyapunov exponent, we explore also changes in other Lyapunov exponents. The motivation lies in the fact that in principle the largest Lyapunov exponent provides only information about the dynamic instability along a certain direction and to gain a complete characterization of a global structure change of phase space requires the full set of Lyapunov exponents and Lyapunov vectors. In Fig. 6 the ϵ dependence of other Lyapunov exponents sampled from the positive branch of the Lyapunov spectrum is presented. Notice that in the near-harmonic regime $\epsilon<\epsilon_{c1}$ all of them follow the same tendency as the largest Lyapunov exponent. As ϵ goes beyond ϵ_{c1} they continue to increase until reaching a maximum around the value $\epsilon_M\approx 1$ and decrease in the high energy regime. Although the general tendency of change in the regime $\epsilon>\epsilon_{c1}$ is the same for all Lyapunov exponents, detailed profiles are quite different from each other, for instance the rates of change in the intermediate- and high-energy regimes. This by considering the variation of the normalized Lyapunov exponents $\lambda^{(\alpha)}(\epsilon)/\lambda^{(\alpha)}(\epsilon_0)$ as presented in Fig. 7 becomes clearly visible. In the near-harmonic regime $\epsilon<\epsilon_{c1}$ all data from different Lyapunov exponents collapse roughly on a single curve. Apart from the largest Lyapunov exponent, the collapse for data of all others continues to $\epsilon_M\approx 1$. The differences between the rescaled Lyapunov exponents increase with further increasing the energy density ϵ.

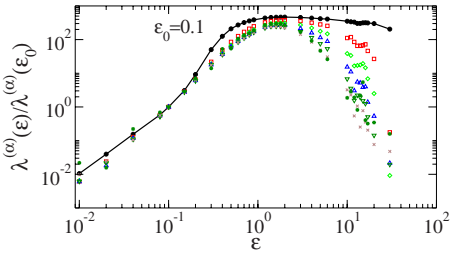

FIG. 7. (Color online) Normalized Lyapunov exponents $\lambda^{(\alpha)}\times(\epsilon)/\lambda^{(\alpha)}(\epsilon_0)$ vs energy density ϵ. Here the more or less arbitrary value $\epsilon_0=0.1$ was chosen. Note that except in the near-harmonic regime $\epsilon<\epsilon_{c1}$ data for different Lyapunov exponents scatter greatly instead of collapsing on a master curve.

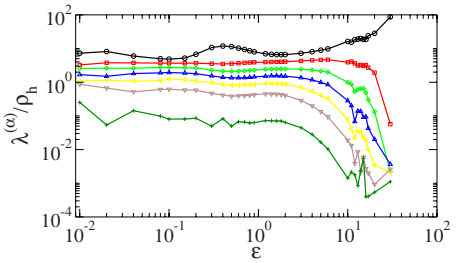

FIG. 8. (Color online) Lyapunov exponents normalized by the entropy density ρ_h vs energy density ϵ for the dynamic XY model.

To show the difference in the energy density dependence of Lyapunov exponents more clearly, we present in Fig. 8 the normalized Lyapunov exponents $\lambda^{(\alpha)}/\rho_h$, where $\rho_h = h_{\mathrm{KS}}/L$ is the density of the Kolmogorov-Sinai entropy. These quantities are expected to be independent of ϵ, if all Lyapunov exponents have exactly identical ϵ dependence. The figure indicates that, the variations of these quantities for all Lyapunov exponents are rather small in the near-harmonic regime $\epsilon < \epsilon_{c1}$. And $\lambda^{(0)}/\rho_h$ attains a local maximum at $\epsilon \approx 0.4$ and bends up as ϵ goes beyond ϵ_M. The variations in other $\lambda^{(\alpha)}/\rho_h$ are still very small in the regime $\epsilon_{c1} < \epsilon < \epsilon_M$ and they bend down one after another in the regime $\epsilon > \epsilon_M$. Notice that the largest Lyapunov becomes already quite large compared to other Lyapunov exponents at $\epsilon = 30$ and the Kolmogorov-Sinai entropy is therefore highly dominated by $\lambda^{(0)}$.

To characterize the fluctuations in Lyapunov instabilities of system trajectories the so-called finite-time Lyapunov exponents (FTLEs) $\lambda_\tau^{(\alpha)}$ are usually used [25]. The finite-time Lyapunov exponent λ_τ represents the average instabilities of trajectory segments of duration τ and it approaches the normal Lyapunov exponent as τ goes to infinity, i.e., $\lim_{\tau\to+\infty}\lambda_\tau = \lambda$. In Fig. 9 we present the standard deviation of FTLEs $\sigma(\lambda_\tau^{(\alpha)})$, a measure of the fluctuations of finite-time Lyapunov exponents λ_τ, with the variation of energy density ϵ. As can be seen from the plot, fluctuations of all FTLEs are quite small and stay constant in the near-harmonic regime $\epsilon < \epsilon_{c1}$. Moreover, in this regime the values of $\sigma(\lambda_\tau^{(\alpha)})$ are roughly identical for all FTLEs, which reflects the isotropic nature of the system dynamics in the near-harmonic regime. With increasing ϵ beyond ϵ_{c1} the quantity $\sigma(\lambda_\tau^{(0)})$ starts to deviate from the other FTLEs and increases with ϵ. With further increasing ϵ the standard deviation $\sigma(\lambda_\tau^{(\alpha)})$ of the other FTLEs also start to increase and deviate from the rest one by one. This splitting process continues to $\epsilon \approx \epsilon_M$. Beyond ϵ_M each FTLE has its own profile of change of σ with ϵ. It seems that with increasing ϵ beyond 30 all $\sigma(\lambda_\tau^{(\alpha)})$ become quite small and tend to be the same except for $\sigma(\lambda_\tau^{(0)})$.

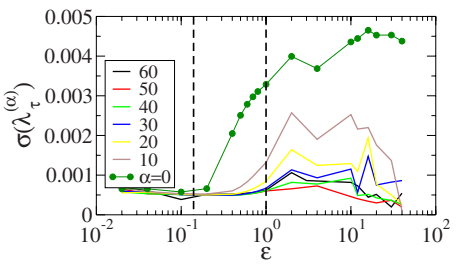

FIG. 9. (Color online) Standard deviations of the finite-time Lyapunov exponents $\sigma(\lambda_\tau^{(\alpha)})$ vs energy density ϵ for the dynamic XY model. Dashed lines indicate the transition values $\epsilon_{c1} = 0.14$ and $\epsilon_M = 1$.

The correspondence between the transitions in Lyapunov exponents and the change in the system dynamics mentioned in Sec. III supports the point of view that these changes in the system dynamics manifest a global change in the geometric structure of phase space. The observed differences in the energy density dependencies of Lyapunov exponents indicate the existence of an alternative scenario of change in the geometric structure of configuration space in contrast to the one for FPU models. The so-called quasi-isotropy assumption has been used in the analytical calculation of the largest Lyapunov exponent [22]. As we pointed out already [36], the success of this seemingly unreasonable assumption in the FPU models has its origin in the strong similarity among the overall profiles of all Lyapunov exponents as the energy density is varied. Our observations here are consistent with such a point of view and explain why in the dynamic XY model there are large differences between numerical results and the analytical calculation of Lyapunov exponent using the quasi-isotropy assumption [22].

B. Transitions in HLMs

We now turn to the characterization of Lyapunov vectors. The focus here will be on the Lyapunov vectors associated with near-zero Lyapunov exponents. Our recent investigation of FPU models [36] has identified the existence of coherent collective structures in these Lyapunov vectors and observed a characteristic change in the significance of HLMs corresponding to the crossover from weak to strong chaos at the SST.

The profile of one typical Lyapunov vector and the corresponding static LV structure factor $S_u^{(\alpha\alpha)}(k)$ is shown in Fig. 10. As can be seen this Lyapunov vector, which is associated with a near-zero Lyapunov exponent, is spatially extended. No clearly visible long wavelength coherent structure, however, can be directly seen from the plot of the profile. To identify the possibly existing vague modes, we adopt the measure of the static LV structure factor defined in Eq. (4). To simplify the notation, we will omit the subscript and superscript of $S_u^{(\alpha\alpha)}(k)$ throughout the remainder of this paper. The corresponding static LV structure factor is presented in panel (b) of Fig. 10. A characteristic feature is the existence of a relatively sharp peak at $k_{\max}$.

We present in Fig. 11 the contour plot of the static LV structure factors for the whole set of Lyapunov vectors. Obviously, the static LV structure factors of Lyapunov vectors associated with near-zero Lyapunov exponents are strongly dominated by certain components with low wave numbers. Moreover, the wave number $k_{\max}$ of the dominant peak approaches $2\pi/L$ gradually as the index α of Lyapunov vectors reaches the center of the Lyapunov spectrum $\alpha = 64$, where the associated Lyapunov exponents become zero. Notice that

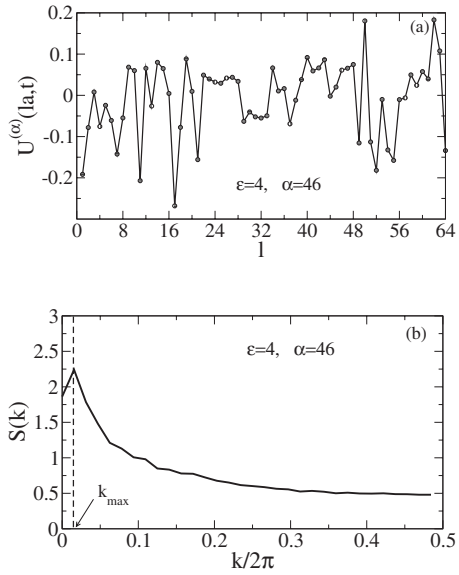

FIG. 10. (a) Profile of a Lyapunov vector with $\alpha=46$ for a randomly selected value of t and (b) the corresponding static LV structure factor $S_u^{(\alpha\alpha)}(k)$ for the dynamic XY model with $\epsilon=4$. The Lyapunov spectrum for $\epsilon=4$ is shown in Fig. 4. Here, $k_{\max}$ is defined as the wave number of the highest peak in the spectrum $S_u^{(\alpha\alpha)}(k)$.

$2\pi/L$ is the smallest nontrivial wave-number allowed by the periodic boundary conditions we used. For a quantitative characterization of the dominance of these peaks, two measures $S(k_{\max})$ and the spectral entropy H_S are used (see Fig. 12). Here $S(k_{\max})$ denotes the height of the dominant peak of the static structure factor of a given Lyapunov vector and the spectral entropy H_S is defined as $H_S \equiv -\Sigma S(k)\ln S(k)$. A small

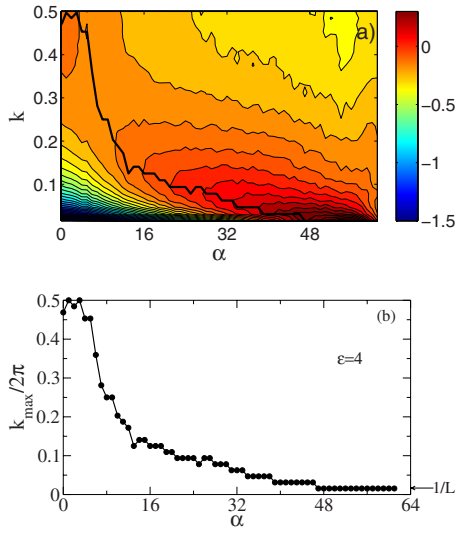

FIG. 11. (Color online) (a) Contour plot of static LV structure factors for the dynamic XY model with $\epsilon=4$. (b) Variation of $k_{\max}$ with the Lyapunov index α. The Lyapunov vectors with $\alpha \approx 64$ are dominated by components with wave numbers comparable to $2\pi/L$, which is the smallest nontrivial wave number permitted by the periodic boundary conditions used. These facts together imply the existence of hydrodynamic Lyapunov modes in this system.

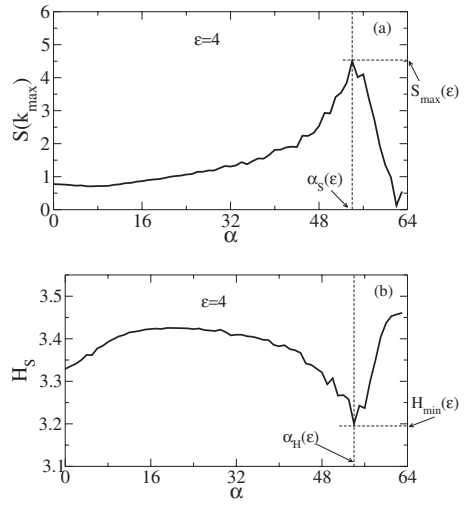

FIG. 12. (a) $S(k_{\max})$ and (b) spectral entropy $H_S \equiv -\Sigma S(k)\ln S(k)$ vs α for the dynamic XY model with $\epsilon=4$. The quantities $S_{\max}(\epsilon)$, $\alpha_S(\epsilon)$, $H_{\min}(\epsilon)$, and $\alpha_H(\epsilon)$ will be used to measure the significance of HLMs.

value of H_S and a large value of $S(k_{\max})$ indicate the existence of a sharp peak in the static LV structure factor under investigation. As can be seen from Fig. 12 both quantities attain their extreme values at $\alpha \simeq 54$. All these numerical results together demonstrate the existence of HLMs in this system.

To facilitate the study of the energy density dependence of HLMs, we use the measures used already in Ref. [36] to quantify the significance of HLMs in a case with given energy density. They are the extreme values $S_{\max}(\epsilon)$ and $H_{\min}(\epsilon)$ as indicated in Fig. 12. Roughly speaking, $S_{\max}(\epsilon)$ represents the height of the highest peak in the static structure factors of all Lyapunov vectors of a case with given ϵ, and $H_{\min}$ measures the significance of this peak. For completeness the normalized index α_H/L, where the spectral entropy is minimal, is also considered.

The variation of these quantities with the energy density ϵ is plotted in Fig. 13. The threshold values $\epsilon_{c1} \simeq 0.14$, $\epsilon_{c2} \simeq 1$ and $\epsilon_M \simeq 10$ mediating the transitions in the system dynamics and in the Lyapunov exponents are marked as dashed lines. Obviously, these significance measures for HLMs also change roughly around these threshold values. As can be seen from the figure, the normalized index α_H/L is rather small in the near-harmonic regime $\epsilon < \epsilon_{c1}$ and in the free-rotation regime $\epsilon > \epsilon_{c2}$, which means that the corresponding Lyapunov exponents are close to the largest Lyapunov exponent. Thus the associated highest peaks do not represent HLMs. In contrast, the values of the normalized indices α_H/L are relatively large and close to 1.0 in the regime $\epsilon_{c1} < \epsilon < \epsilon_{c2}$. A value of α_H of order L implies that near-zero Lyapunov exponents are associated with strong peaks in the structure function. Therefore the associated highest peaks represent certain HLMs. In comparison with Figs. 21 and 22 of Ref. [36] one can see that the scenario of change in these significance measures at ϵ_{c1} is quite similar to that in the FPU-β model [36]. This may be due to the fact that the parametric resonance is the only (dominant) mechanism of

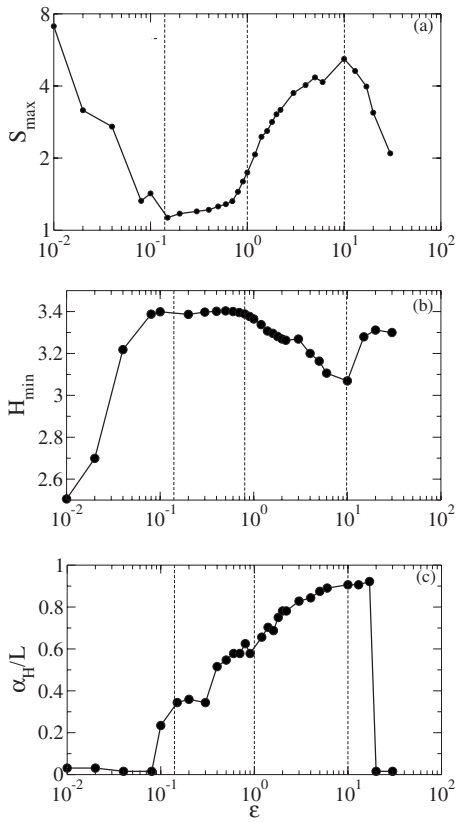

FIG. 13. (a) $S_{\max}(\epsilon)$, (b) $H_{\min}$, and (c) the normalized index α_H/L vs ϵ for the dynamic XY model. Here, the threshold values of the energy density for transitions in the Lyapunov spectrum are shown as dashed lines. Notice the change in the behavior of these quantities at these threshold values.

dynamical instability there. As already mentioned the occurrence of negative curvature serves as an additional source of dynamical instabilities in the XY model [22]. With increasing ϵ from ϵ_{c1} the probability of occurrence of negative curvatures increases. The increase of $S_{\max}(\epsilon)$ becomes even faster with increasing ϵ beyond the threshold value ϵ_M and the descent of $H_{\min}(\epsilon)$ becomes slower correspondingly since the occurrence of negative curvatures seems to become the dominant mechanism of dynamical instability. The occurrence of negative curvatures enhances the chaoticity of our system and leads to the appearance of more significant HLMs consequently. Above $\epsilon=\epsilon_{c2}$ the dynamics becomes more regular again, and therefore ϵ_{c2} is interpreted as SST mediating a transition from weak chaotic ($\epsilon>\epsilon_{c2}$) to strong chaotic ($\epsilon_M<\epsilon<\epsilon_{c2}$) motion characterized by a negative curvature of the ambient manifold. This explains the decrease of $S_{\max}$ and the corresponding increase of $H_{\min}$ as the energy density is increased beyond ϵ_{c2}. Notice that the crossover points of these significance measures of HLMs all lie in the regimes around the threshold energy densities of corresponding transitions in the Lyapunov spectrum. This implies that both the transitions in the Lyapunov spectrum and in the Lyapunov vectors at the SSTs are possibly manifestations of the same geometric changes in the structure of phase space. To be specific, the four dynamic regimes WL ($\epsilon<\epsilon_{c1}$), SL ($\epsilon_{c1}<\epsilon<\epsilon_M$), SR ($\epsilon_M<\epsilon<\epsilon_{c2}$), and WR ($\epsilon>\epsilon_{c2}$) and the corresponding transitions are manifested not only in the Lyapunov exponents but also in the character of the Lyapunov vectors. Compared to the cases of the FPU models [36] the scenario of change in the dynamic XY model is obviously more complex.

V. SUMMARY AND DISCUSSION

In this paper, we investigated the energy density dependence of Lyapunov exponents and HLMs in the dynamic XY model. The scenario of change in the Lyapunov exponents in this model is different from that of FPU models. To be precise, the profiles of change of all Lyapunov exponents with varying energy density are different from each other except in the near-harmonic regime. HLMs are demonstrated to exist in this system. The significance measures of HLMs change significantly corresponding to transitions in the Lyapunov exponents. These facts support the anticipation that the transitions in the system dynamics at the SSTs manifest global changes in the geometric structure of phase space.

In contrast to the FPU models and the lattice φ^4 model the occurrence of negative curvatures serves as an additional source of dynamical instabilities in the dynamical XY model. This may be the very reason why the scenario of change in Lyapunov characteristics of the dynamic XY model is different from and more complex than that of the formers.

In the literature simple measures such as the largest Lyapunov exponent and the scalar curvature or the Ricci curvature are frequently used to characterize the geometric change in the phase space of high-dimensional Hamiltonian systems. As pointed out in Ref. [19], one may obtain "some synthetic indicator of chaos similar to the largest Lyapunov exponent" by using the scalar or Ricci curvatures. In systems such as the FPU models and the lattice φ^4 models all Lyapunov exponents contain nearly the same information as the largest Lyapunov exponent. Therefore the use of only the largest Lyapunov exponent or the scalar curvature or the Ricci curvatures seems to be sufficient. Our current investigation shows that the scenario of change in the geometric structure of phase space is not always as simple as in the FPU models. In general each Lyapunov exponent encodes different information about the dynamical instability along a certain direction. In principle, using all of them together, or equivalently the Riemannian curvature tensor, provides a complete characterization of the dynamical instability of the considered systems. Our results thus restrict the use of only such crude measures to characterize transitions in the dynamics of high-dimensional Hamiltonian systems.

Recently the geometric picture of Hamiltonian chaos has been used to characterize also transitions in the dynamics of biomacromolecules such as protein folding [42,43]. The energy landscape of these macromolecules is in general quite complex and the functionally relevant motions of these macromolecules are often strongly anharmonic. For instance, escaping over potential barriers turns out to be an important ingredient of the interwell motion of these macromolecules. Therefore, segments of the energy landscape with negative curvatures are encountered frequently. We expect that the

scenario of change in the dynamics of these systems should be similar to what we reported for the dynamic *XY* model in some respects.

ACKNOWLEDGMENTS

Support from the Deutsche Forschungsgemeinschaft (DFG Grant No. Ra416/6-1), computing time from NIC Jülich, and algorithmic support from Gudula Rünger and Michael Schwind are gratefully acknowledged.

APPENDIX: SCENARIO OF CHANGE OF LYAPUNOV EXPONENTS IN THE LATTICE φ^4 MODEL

In this appendix we show the change in the scaling behavior of the energy density dependence of Lyapunov exponents in the lattice φ^4 model [14]. The Hamiltonian of this model reads

$$H = \sum_{l=1}^{L} \left[\frac{p_l^2}{2} + (\varphi_{l+1} - \varphi_l)^2 + \frac{1}{2} m^2 \varphi_l^2 + \frac{1}{4} \mu \varphi_l^4 \right], \quad \text{(A1)}$$

where φ_l denotes the displacement of the lth particle from its equilibrium position, $p_l \equiv \dot{\varphi}$ is the conjugate momentum. Other quantities have the same meaning as in Eq. (1) and the constants take the values $m=0.1$ and $\mu=0.01$.

Notice that the existence of an on-site potential in the lattice φ^4 model breaks the translational symmetry in φ. Therefore, no HLMs are expected in this system. Numerical simulations confirm this point and we show below the energy density dependence of Lyapunov exponents.

As can be seen in Fig. 14, the scenario of change in Lyapunov exponents in the lattice φ^4 model is rather similar to that of the FPU models [36]. Profiles of the energy density dependence of all Lyapunov exponents are quite similar, i.e., the speed of increase changes smoothly in the regime around the SST threshold value $\epsilon_c=0.5$ [14]. The collapse of rescaled data $\lambda^{(\alpha)}(\epsilon)/\lambda^{(\alpha)}(\epsilon_0)$ is, however, not as perfect as in the FPU models. This is also evident in the variation of $\lambda^{(\alpha)}(\epsilon)/\rho_h$ with the energy density ϵ shown in the panel (c). These results suggest that the change in the geometric structure of phase space at the SST in the lattice φ^4 model is similar to that of the FPU models but different from that of the dynamic *XY* model. Note that in a study of the time scales to energy equipartition a comparison between the two models was made [44]. The reported transitions in the equipartition time should be related to the change in the scaling of Lyapunov exponents we observed here. On the basis of the current different parameter settings a detailed comparison cannot be made, but may be an interesting point for future research.

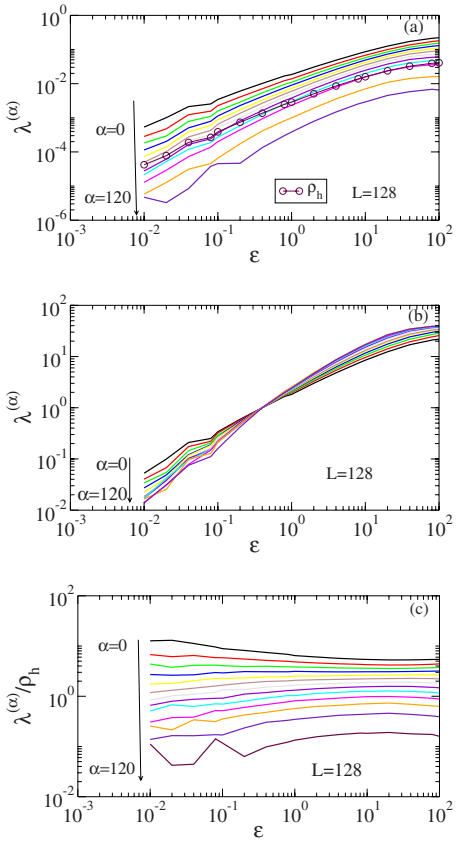

FIG. 14. (Color online) Energy density dependence of (a) Lyapunov exponents $\lambda^{(\alpha)}(\epsilon)$ sampled from the positive branch of the Lyapunov spectrum, (b) normalized Lyapunov exponents $\lambda^{(\alpha)}(\epsilon)/\lambda^{(\alpha)}(\epsilon_0)$ with $\epsilon_0=0.4$, and (c) Lyapunov exponents normalized by the Kolmogorov-Sinai entropy density $\lambda^{(\alpha)}/\rho_h$ for the lattice ϕ^4 model.

[1] N. S. Krylov, *Works on the Foundations of Statistical Mechanics* (Princeton University Press, Princeton, NJ, 1979).
[2] P. Gaspard, *Chaos, Scattering, and Statistical Mechanics* (Cambridge University Press, Cambridge, UK, 1998).
[3] J. P. Dorfman, *An Introduction to Chaos in Nonequilibrium Statistical Mechanics* (Cambridge University Press, Cambridge, UK, 1999).
[4] D. J. Evans and G. P. Morriss, *Statistical Mechanics of Nonequilibrium Liquids* (Academic, New York, 1990).
[5] W. G. Hoover, *Computational Statistical Mechanics* (Elsevier, New York, 1991).
[6] W. G. Hoover, *Time Reversibility, Computer Simulation, and Chaos* (World Scientific, Singapore, 1999).
[7] E. Fermi, J. Pasta, and S. Ulam (with M. Tsingou), Los Alamos Report No. LA-1940 (1955), in *Collected Papers of Enrico Fermi*, edited by E. Segré (University of Chicago, Chicago, 1965), Vol. 2, p. 978.
[8] See, for example, Chaos **15** (2005), special issue on the FPU problem.
[9] A. N. Kolmogorov, Dokl. Akad. Nauk SSSR **98**, 527 (1954); J. Moser, Nachr. Akad. Wiss. Goett. II, Math.-Phys. Kl. **1**, 1 (1962); V. I. Arnold, Russ. Math. Surveys **18**, 9 (1963).

[10] F. M. Izrailev and B. V. Chirikov, Dokl. Akad. Nauk SSSR **166**, 57 (1966) [Sov. Phys. Dokl. **11**, 30 (1966)].
[11] P. Bocchieri, A. Scotti, B. Bearzi, and A. Loinger, Phys. Rev. A **2**, 2013 (1970).
[12] R. Livi, M. Pettini, S. Ruffo, M. Sparpaglione, and A. Vulpiani, Phys. Rev. A **28**, 3544 (1983); **31**, 1039 (1985); R. Livi, M. Pettini, S. Ruffo, and A. Vulpiani, Phys. Rev. A **31**, 2740 (1985).
[13] H. Kantz, Physica D **39**, 322 (1989).
[14] M. Pettini and M. Cerruti-Sola, Phys. Rev. A **44**, 975 (1991); M. Pettini and M. Landolfi, *ibid.* **41**, 768 (1990).
[15] For a review of the current state see, for example, M. Pettini, L. Casetti, M. Cerruti-Sola, R. Franzosi, and E. G. D. Cohen, Chaos **15**, 015106 (2005).
[16] D. Escande, H. Kantz, R. Livi, and S. Ruffo, J. Stat. Phys. **76**, 605 (1994).
[17] K. Yoshimura, Physica D **104**, 148 (1997).
[18] M. Cerruti-Sola, M. Pettini, and E. G. D. Cohen, Phys. Rev. E **62**, 6078 (2000).
[19] M. Pettini, Phys. Rev. E **47**, 828 (1993).
[20] L. Casetti and M. Pettini, Phys. Rev. E **48**, 4320 (1993).
[21] L. Casetti, R. Livi, and M. Pettini, Phys. Rev. Lett. **74**, 375 (1995).
[22] L. Casetti, C. Clementi, and M. Pettini, Phys. Rev. E **54**, 5969 (1996).
[23] L. Casetti, M. Pettini, and E. G. D. Cohen, Phys. Rep. **337**, 237 (2000).
[24] H. A. Posch and R. Hirschl, in *Hard Ball Systems and the Lorentz Gas*, edited by D. Szàsz (Springer, Berlin, 2000), p. 279.
[25] C. Forster, R. Hirschl, H. A. Posch, and Wm. G. Hoover, Physica D **187**, 294 (2004).
[26] J.-P. Eckmann and O. Gat, J. Stat. Phys. **98**, 775 (2000).
[27] S. McNamara and M. Mareschal, Phys. Rev. E **64**, 051103 (2001); M. Mareschal and S. McNamara, Physica D **187**, 311 (2004).
[28] A. S. de Wijn and H. van Beijeren, Phys. Rev. E **70**, 016207 (2004).
[29] T. Taniguchi and G. P. Morriss, Phys. Rev. E **65**, 056202 (2002); **68**, 026218 (2003); Phys. Rev. Lett. **94**, 154101 (2005).
[30] J.-P. Eckmann, C. Forster, H. A. Posch, and E. Zabey, J. Stat. Phys. **118**, 813 (2005).
[31] H. L. Yang and G. Radons, Phys. Rev. E **71**, 036211 (2005).
[32] G. Radons and H. L. Yang, e-print arXiv:nlin.CD/0404028.
[33] C. Forster and H. A. Posch, New J. Phys. **7**, 32 (2005).
[34] H. L. Yang and G. Radons, Phys. Rev. E **73**, 016202 (2006); **73**, 016208 (2006).
[35] H. L. Yang and G. Radons, Phys. Rev. Lett. **96**, 074101 (2006).
[36] H. L. Yang and G. Radons, Phys. Rev. E **73**, 066201 (2006).
[37] P. Butera and G. Caravati, Phys. Rev. A **36**, 962 (1987).
[38] C. Giardiná, R. Livi, A. Politi, and M. Vassalli, Phys. Rev. Lett. **84**, 2144 (2000).
[39] O. V. Gendelman and A. V. Savin, Phys. Rev. Lett. **84**, 2381 (2000); A. V. Savin and O. V. Gendelman, Phys. Solid State **43**, 355 (2001).
[40] Both the standard RK4 algorithm and a symplectic version are used for our simulations reported here. The symplectic version is according to J. M. Sanz-Serna and M. P. Calvo, *Numerical Hamiltonian Problems* (Chapman and Hall, London, 1994).
[41] G. Benettin, L. Galgani, and J. M. Strelcyn, Phys. Rev. A **14**, 2338 (1976); G. Benettin, L. Galgani, A. Giorgilli, and J. M. Strelcyn, Meccanica **15**, 9 (1980); **15**, 21 (1980); I. Shimada and T. Nagashima, Prog. Theor. Phys. **61**, 1605 (1979).
[42] A. Mossa, M. Pettini, and C. Clementi, Phys. Rev. E **74**, 041805 (2006).
[43] L. N. Mazzoni and L. Casetti, Phys. Rev. Lett. **97**, 218104 (2006).
[44] J. De Luca and A. Lichtenberg, Phys. Rev. E **66**, 026206 (2002).